Adsorption of Basic Magenta on Graphene Oxide-modified Sugarcane Bagasse

Renjin Gao,[a,b] Xiaoting Shen,[a] and Liwei Wang [a,b,c,*]

A novel adsorbent was prepared using sugarcane bagasse modified with graphene oxide. The adsorbent was characterized using Fourier transform infrared spectroscopy, thermogravimetric analysis, scanning electron microscopy, and X-ray diffraction analyses. The adsorption of basic magenta on bagasse and graphene oxide-modified bagasse was systematically studied. The effects of initial concentration, adsorption time, adsorption temperature, and the amount of the adsorbent on the adsorption capacity were examined. Adsorption isotherms were described using both the Langmuir and Freundlich models. It was found that the Langmuir model fit well with the experimental data. The results revealed that the adsorption percentage of basic magenta increased from 55.4% to 99.5% under optimal adsorption conditions. The maximum absorption capacity was 145 mg/g.

Keywords: Bagasse; Graphene oxide; Basic magenta; Adsorption

Contact information: a: Ocean College, Minjiang University, Fuzhou, Fujian 350108 China; b: Fujian Engineering and Research Center of New Chinese Lacquer Materials, Fuzhou 350108, China; c: Fujian Key Laboratory of Textile Fiber and Materials, Fuzhou 350108, China;
** Corresponding author: wlw@mju.edu.cn*

INTRODUCTION

The toxic pollutants in water bodies are an environmental problem of recent decades, and many efforts have been made to solve this problem (Vinod *et al.* 2012). Textile industries discharge large volumes of water containing synthetic dyes, so they are significant sources of pollution (Crini 2006). Dyes are recalcitrant to photochemical and biological degradation, and their degradation products may be toxic, in some cases including mutagens and carcinogens (Garg *et al.* 2004; Al-Aoh *et al.* 2014). In particular, basic magenta (BM) is a cationic dye and used extensively in wool, acrylic, silk, and nylon dyeing due to its bright color, high solubility, and simple application process. Under anaerobic conditions it can decompose into carcinogenic aromatic amines that can cause allergic dermatitis, skin irritation, and even cancer (Srinivasan and Viraraghavan 2010). Therefore, the development of efficient, economical, and sustainable dye removal processes is of great importance (He *et al.* 2013).

Numerous dye removal techniques, such as adsorption, advanced oxidation processes, coagulation, electrochemical treatment, flocculation, membrane filtration, ozonation, radiolysis, and reverse osmosis, have been applied to treat textile wastewater (Hatem *et al.* 2014; Fideles *et al.* 2018). Among these methods, adsorption has some advantages for wastewater treatment, such as low cost, flexibility and simplicity of design, and ease of operation (Gupta *et al.* 2013; Yagub *et al.* 2014; Zhou *et al.* 2016). Furthermore, adsorption also does not result in the formation of harmful substances. Therefore, the development of new adsorbent materials has attracted many researchers' attention.

Sugarcane bagasse (SCB) is produced by the sugar and alcohol industries in China, India, and Brazil. According to the statistical data of the Food and Agriculture Organization of the United Nations (FAO), approximately 1900 million metric tons of sugarcane stalks were produced in 2014. As a renewable and abundant source of environmental waste, bagasse is usually used to burn as fuel for boilers in sugar refineries or pulped to produce paper. However, higher-valued uses of SCB need to be explored (Xiong 2018). Sugarcane bagasse is mainly composed of cellulose (40% to 45%), hemicellulose (25% to 35%), and lignin (15% to 35%) (Gnansounou 2010). There are many functional groups on their surface, such as -COOH and -OH, which provide the active sites for the adsorption of the dyes. Bagasse has been used effectively as an adsorbent for the removal of different pollutants from aqueous solutions; however, its application has been limited due to its low absorption ability, poor mechanical properties, and loose structure (Li *et al.* 2017, 2018; Sun *et al.* 2018).

Graphene is an interesting functional material due to its high electrical conductivity, high intrinsic mobility, and high chemical and thermal stability (Allen *et al.* 2010), and high specific surface area (2630 m^2/g) (Mhamane *et al.* 2011). These features make graphene and their composite potentially applicable to many research fields, such as in the form of supercapacitors, metal oxide functional nanocomposites, and for catalysis (Allen *et al.* 2010). Graphene oxide is a derivate of graphene, and their structures are similar. However, graphene oxide sheets are covered with epoxy, hydroxyl, and carboxyl groups, which provide excellent aqueous dispersity, acidic properties, and tremendous opportunities for access to functionalized graphene-based materials. Lignin-cellulose functionalized graphene (LCG) sponge was synthesized using GO and sugarcane waste powder in presence of natural latex, and it was found that its absorption ability was enhanced for removal of oil and organic solvent (Kulal *et al.* 2019). A polylactic acid-based cerium dioxide-GO composite was developed by means of a sol-gel technique, and its adsorption ability of methyl orange (MO) was improved. It could be used as a suitable electrode material for the removal of MO dye from wastewater (Mohammad *et al.* 2019). A three-dimensional chitosan-graphene composite was synthesized and was used for the removal of reactive black 5 due to its large specific surface area (Cheng *et al.* 2018). Bagasse was also used to reduce GO, and the synthesized bagasse-based rGO was applied to remove dye wastewater (Li *et al.* 2018; Gan *et al.* 2019). Research related to the usage of GO in adsorption of dyes has been reviewed by Sophia *et al.* (2019).

In this article, a novel adsorbent was prepared using graphene oxide-modified sugarcane bagasse and used for the removal of basic magenta. The influence of solution temperature, adsorption time, adsorbent dosage, and initial dye concentration on the adsorption process were studied, which could provide useful information for the further application of sugarcane bagasse.

EXPERIMENTAL

Materials

Sugarcane bagasse was bought from a local market in Fuzhou, Fujian province, China. It was soaked in distilled water, washed, and dried until further use. It was ground into powder and passed through a 200-mesh screen.

Multilayered graphene oxide (purity > 95%) was supplied by Tanfeng Scientific Technology Co., Ltd. (Suzhou, China). Basic magenta, sodium hydroxide (NaOH), and

urea were bought from Xilong Scientific Co., Ltd. (Guangdong, China). The chemicals used in this study were analytically pure.

Preparation of sugarcane bagasse modified by graphene oxide

A total of 5 g of treated sugarcane bagasse powder was added into 100 mL of 6% NaOH solution, and the temperature was kept at 60 °C for 1.5 h. Afterwards, it was left to cool to room temperature, then vacuum filtered, and washed with distilled water several times until the solution was neutral. The solid was oven-dried at 120 °C for 2 h and light-yellow sugarcane bagasse fiber was obtained.

Distilled water, NaOH, and urea were mixed in the ratio of 85:10:5, and solution I was obtained. Solution I was kept at -10 °C for 8 h. Then, 1 g prepared sugarcane bagasse fiber was dissolved in 200 mL solution I at 0 °C under stirring for 6 h. After that, the temperature of the mixture was raised to room temperature, and 0.5% basic sugarcane bagasse fiber solution was obtained and noted as solution II.

A total of 25 mL of 5 mg/mL graphene oxide suspension was added to solution II and the mixture was ultrasonically oscillated for 30 min. Then, the suspension was filtered and washed with distilled water until the solution was neutral. The wet solid was oven-dried at 60 °C and the graphene oxide-modified sugarcane bagasse composite was finally obtained.

Methods

Characterization of adsorbent

The Fourier transform infrared (FTIR) spectra were obtained using a Nicolet MPIR 8400S spectrometer (Shimadzu Corporation, Kyoto, Japan). A total of 32 scans were accumulated for each spectrum at a resolution of 4 cm^{-1} in the region of 3700 to 700 cm^{-1} using KBr pellets.

The thermal stability was tested using a STA 449F3 thermogravimetric analyzer (NETZSCH, Bavaria, Germany). The carrier gas and protective gas were highly pure nitrogen with a flow rate of 20 mL/min and 20 mL/min, respectively. The temperature was set from 30 °C to 500 °C with a heating rate of 10 °C/min.

Scanning electron microscopy (SEM) images were obtained using a field emission scanning electronic microscope (SU8000; Hitachi, Tokyo, Japan) at an acceleration voltage of 2.0 kV.

The crystal structure was characterized using a Miniflex 600 X-ray diffractometer (XRD; Rigaku, Tokyo, Japan). The scanning range was set at the angle range of 3° to 85°.

Adsorption of adsorbent

A typical procedure used in adsorption studies is as follows: 0.03 g adsorbent was added into a bottle with 50 mL of 30 mg/L basic magenta solution. The bottle was then kept in an incubator shaker for 90 min at 60 °C. After reaching the equilibrium, the sample was centrifuged, and the clear solution was removed for measurement. The concentration of basic magenta was determined *via* spectrophotometric analysis at 548 nm based on standard curve, which was drawn by the absorbance of the solutions with known concentrations. The adsorption percentage of the adsorbent was calculated according to Eq. 1,

$$\eta\ (\%) = [(C_0 - C_t)\ /\ C_0] \times 100 \quad (1)$$

where n is the adsorption percentage (%) of basic magenta at time t, and C_0, and C_t are the concentration of the dye solutions initially and at time t (mL/g), respectively. The adsorption capacity was calculated according to Eq. 2,

$$q = [(C_0 - C_t)V / W] \quad (2)$$

where q is the adsorption capacity (mg/g), V is the volume of the dye solution (L), and W is the weight of the absorbent (g).

The effect of adsorbent amount, adsorption temperature, adsorption duration, and initial concentration of basic magenta on the adsorption was systematically investigated.

RESULTS AND DISCUSSION

Characterization of the Adsorbent

XRD analysis

The XRD pattern of untreated sugarcane bagasse (SCB), graphene oxide/ sugarcane bagasse (GO/SCB), and graphene oxide (GO) was recorded to study the changes in crystallinity of the fibers during the course of modification (Fig. 1). The crystalline nature of cellulose was revealed with major peaks at 15.85° and 22.15° from the XRD patterns of raw bagasse. The high intensity diffraction peak of GO appears near 2θ = 10.65° due to high crystallinity of GO (Lee and Kim 2014). However, after the modification, the peak at 2θ = 15.85° had disappeared, while the peak of GO had shifted to 2θ=10.83° and the peak of SCB had shifted to 2θ = 21.25°. Moreover, a decrease in the intensity of the peaks at 10.83 and 21.25 was observed. This result further indicated effective chemical modification of cellulose resulting in a decrease in the crystallinity of the fibers.

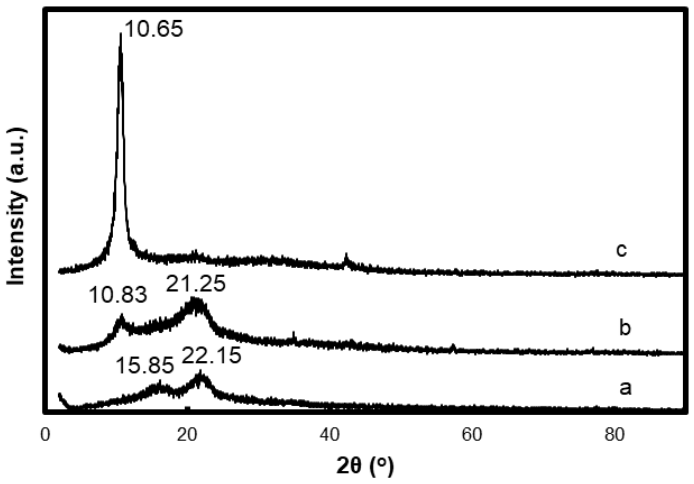

Fig. 1. XRD patterns of untreated sugarcane bagasse (a), graphene oxide/sugarcane bagasse (b), and graphene oxide (c)

FTIR spectral analysis

The FTIR spectra of the untreated sugarcane bagasse (SCB), graphene oxide/ sugarcane bagasse (GO/SCB), and graphene oxide (GO) are depicted in Fig. 2. For GO, a strong and wide band was observed at 3170 cm^{-1} due to the O-H stretching vibration. The narrow peak at 1720 cm^{-1} was caused by the C=O stretching of carboxylic acid (COOH).

The bonds at around 1620 cm^{-1} and 1040 cm^{-1} can be attributed to the presence of C=C and C-O (Nethravathi and Rajamathi 2008).

The spectrum of SCB had an absorption band at 3340 cm^{-1} corresponding to stretching vibrations of hydroxyl (-OH) groups. The bands at 2890 cm^{-1} and 1730 cm^{-1} were assigned to the C=O stretching vibration of acetyl and uronic ester groups in hemicellulose or ester of ferulic and p-coumeric acid in lignin. The peaks at 1600 cm^{-1} and 1240 cm^{-1} represent characteristic aromatic C=C stretching in lignin. The absorption band at 1030 cm^{-1} is due to pyranose ring skeletal vibration (Lee and Kim 2014). In contrast, the spectrum of GO/SCB had absorption bands located at 3340 cm^{-1}, 2890 cm^{-1}, and 1030 cm^{-1}, which were suggestive of a typical cellulose structure. The complete disappearance of peaks at 1730 cm^{-1} and 1240 cm^{-1} shows removal of hemicelluloses and lignin from the bagasse during the modification (Sun *et al.* 2018).

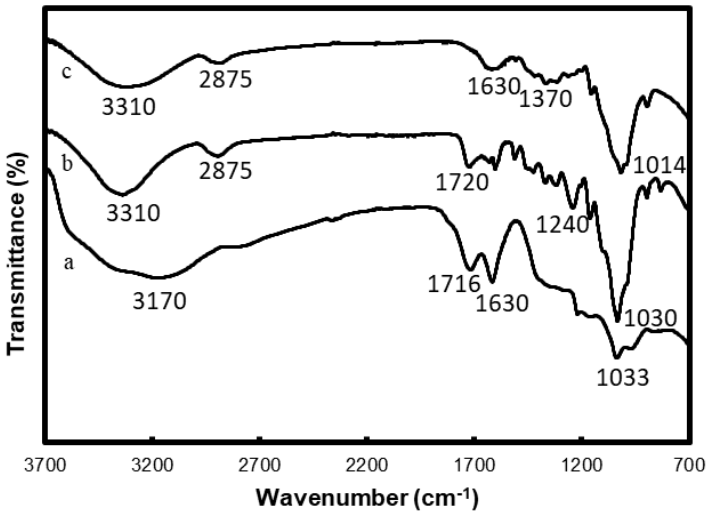

Fig. 2. FTIR spectra of graphene oxide (a), untreated sugarcane bagasse (b), and graphene oxide/sugarcane bagasse (c)

SEM analysis

Figures 3a and 3b represent the SEM photographs of untreated sugarcane bagasse (SCB) and graphene oxide/sugarcane bagasse (GO/SCB). There was a clear change in the morphology of the bagasse after modification. The surface of SCB was smooth. However, after modification, the surface of GO/SCB was coarse and more pores were observed due to the presence of GO on the surface of SCB. There were plenty of hydroxyl groups in the cellulose, resulting in a hydrogen bond between cellulose molecules. Bonding between GO and SCB only took place on the surface due to the hydrogen bond and high crystallinity of the cellulose (Li *et al.* 2017). In contrast, there were some oxygen-containing groups on the surface of GO, which can form the non-covalent bonds with the hydroxyl group of cellulose of the SCB (Fideles *et al.* 2018). Both hydrogen bonds and non-covalent bonds contributed to the properties of the surface, which was beneficial to the increase in the absorption ability.

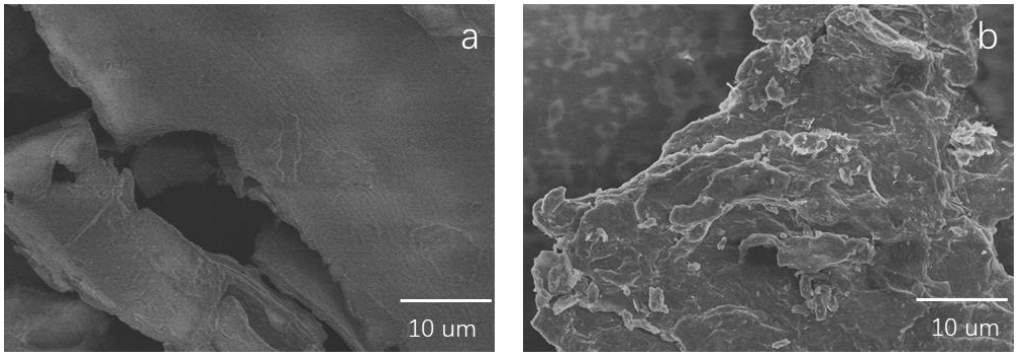

Fig. 3. SEM micrograph of untreated sugarcane bagasse (a) and graphene oxide/sugarcane bagasse (b)

Thermal analysis

Figure 4 presents the thermogravimetric analysis (TGA) curves of the untreated sugarcane bagasse (SCB) and the graphene oxide/sugarcane bagasse (GO/SCB). In the stage at 30 to 120 °C, a weight loss of approximately 10% resulted from the loss of the absorbed water. In the range of 120 to 260 °C, the weight loss was 15% and 20% for SCB and GO/SCB, respectively, which was attributed to the decomposition of oxygen-containing groups, such as hydroxyl, carboxyl, and epoxy, under high temperature (Li *et al.* 2017). With increased temperature, the weight fell dramatically; a weight loss of 64% for GO/SCB and 80% for SCB was observed. This was due to the pyrolysis of cellulose with the release of the gas. The thermal stability of the sugarcane bagasse was increased due to the modification of graphene oxide.

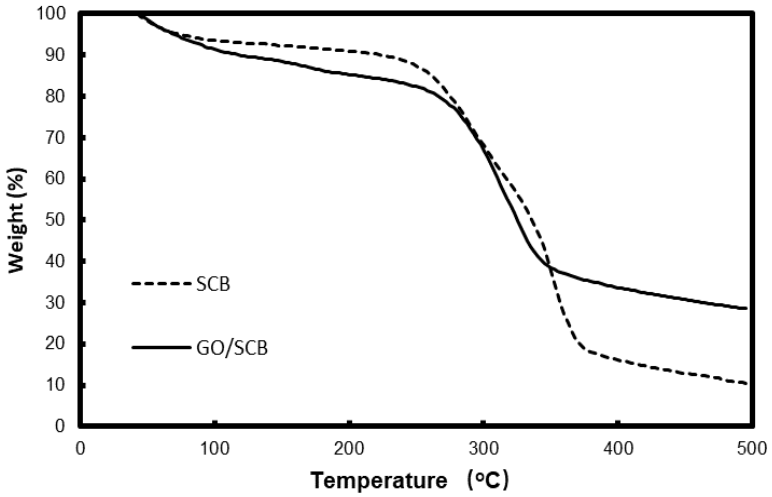

Fig. 4. TGA curves of untreated sugarcane bagasse (SCB) and graphene oxide/sugarcane bagasse (GO/SCB)

Study of the Adsorption

Comparison of adsorption ability

Table 1 shows the adsorption percentage of SCB and GO/SCB for BM. It was observed that SCB showed lower efficiency (55.4%) for the removal of BM than the GO/SCB (99.5%). This could have been explained by the fact that SCB contained fewer adsorption sites. In contrast, GO/SCB showed a high adsorption percentage, indicating that

SCB modification with GO increased the adsorption sites and improved the adsorption performance.

Table 1. Comparison on Adsorption Efficiency of BM on SCB and GO/SCB

Sample	SCB	GO/SCB
Adsorption efficiency (%)	55.4	99.5

Effect of the temperature on adsorption

The effect of the temperature on the adsorption of BM onto GO/SCB was examined at 30, 40, 50, 60, 70, and 80 °C. The results are presented in Fig. 5. The results demonstrate that the adsorption capacity of the GC/SCB increased with increasing temperature of the solution, which meant that the processes were endothermic. This was attributed to the increase in the mobility of BM due to the increased solution temperature. Thus, an adequate energy may be also required for an additional number of molecules to undergo an interaction with the active site at the surface (Hameed and Ahmad 2009). Moreover, rising temperature may cause swelling for the internal structure of these adsorbents, which enable extra dye molecules to penetrate them (Al-Aoh *et al.* 2014).

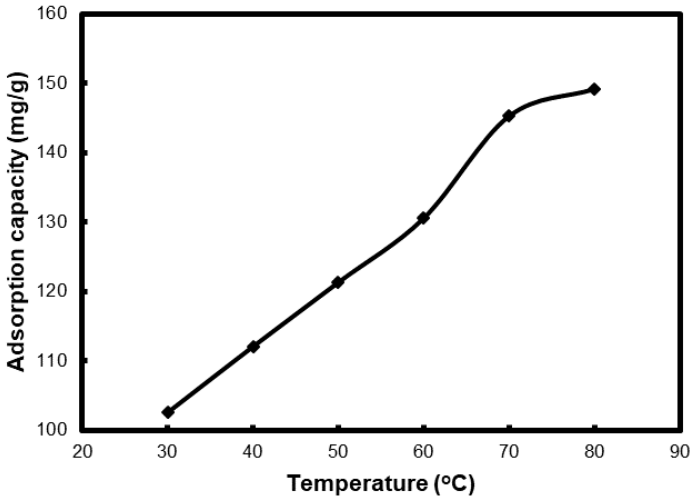

Fig. 5. Adsorption capacity of graphene oxide/sugarcane bagasse change with temperature

Effect of the amount of adsorbent on adsorption

The effect of the dosage of GO/SCB on the adsorption performance is shown in Fig. 6. Adsorption ability increased with the amount of GO/SCB linearly until 0.03 g of GO/SCB was used. More adsorbent resulted in more adsorption sites, resulting in high adsorption performance. When the mass of GO/SCB was 0.03 g, the adsorption performance reached maximum and almost all of the dye was removed.

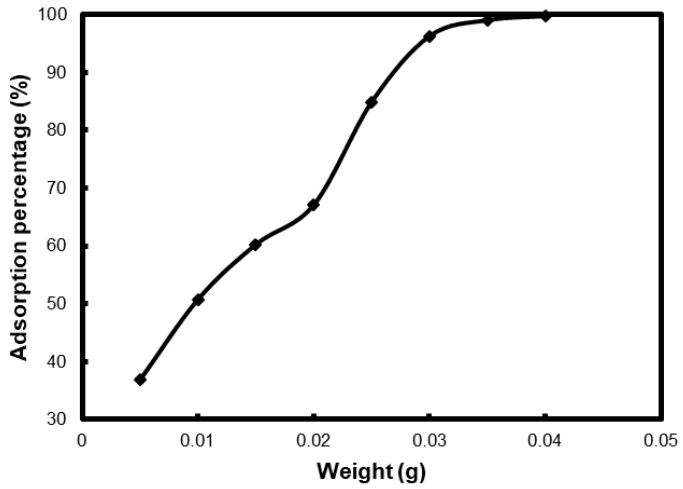

Fig. 6. Adsorption capacity of graphene oxide/sugarcane bagasse change with the weight of adsorbent

Adsorption kinetic study

The change of the adsorption capacity with time is presented in Fig. 7. The adsorption capacity remarkable increased until 120 min, indicating that the few adsorption sites was exposed to the dyes. Thus, the adsorption time was chosen at 120 min.

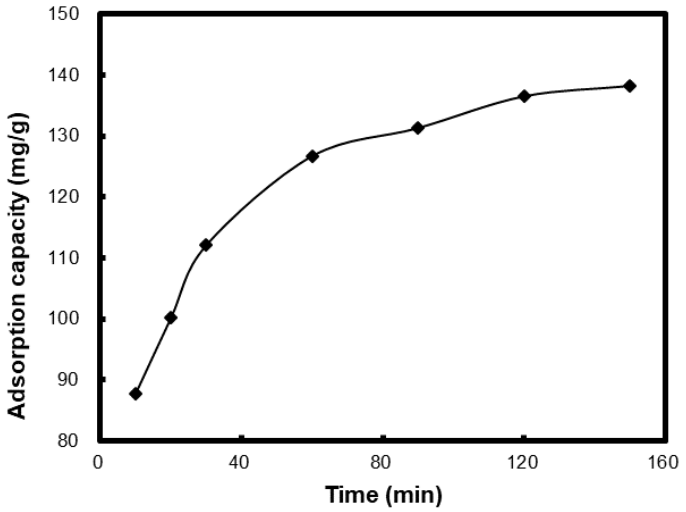

Fig. 7. The variation of the adsorption capacity of graphene oxide/sugarcane bagasse with time

To examine the adsorption kinetics, the adsorption studies were applied to two models, the Lagergren pseudo-first-order and pseudo-second-order equations (Eqs. 3 and 4) (Tan *et al.* 2007),

$$\ln(q_e - q_t) = lnq_e - k_1 t \quad (3)$$

$$\frac{t}{q_t} = \frac{1}{k_2 q_e^2} + \frac{t}{q_e} \quad (4)$$

where q_e is the adsorption capacity (mg/g) at equilibrium, q_t is the adsorption capacity (mg/g) at time t, k_1 and k_2 are the adsorption rate constants (min^{-1}, g/mg min^{-1}, respectively) of the pseudo-first order reaction and pseudo-second order reactions, respectively. The values of k_1 and q_e (Eq. 3) were calculated from the slopes and intercepts of the plots of $\ln(q_e - q_t)$ *vs*. t, which are presented in Fig. 8. The q_e (Eq. 4) and k_2 were calculated from the slopes and intercepts of the plots of t/q_t *vs*. t, which are demonstrated in Fig. 9. The calculated values of kinetic parameters and their corresponding correlation coefficient value are listed in Table 2.

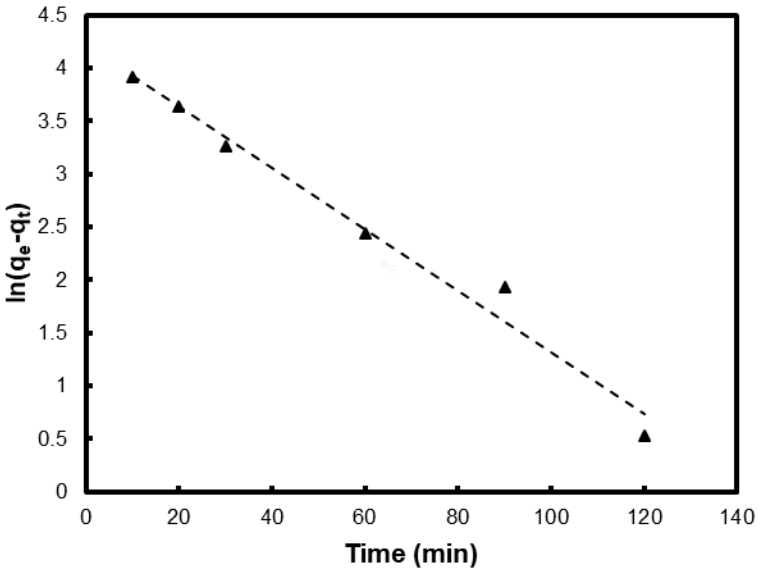

Fig. 8. Pseudo-first-order kinetics model for the adsorption of BM on GO/SCB

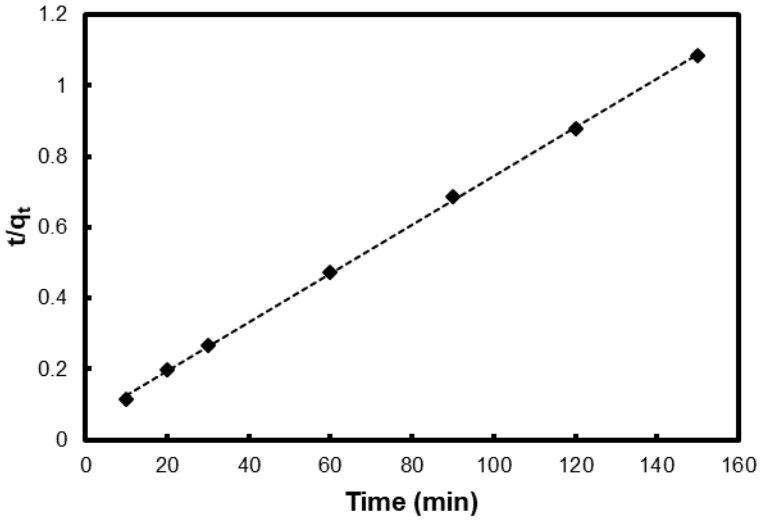

Fig. 9. Pseudo-second-order kinetics model for the adsorption of BM on GO/SCB

It was observed from Table 2 that the experimental data matched the pseudo-second-order model (R^2 = 0.9996) close to 1.0, which was better than the pseudo-first-

order model (R^2 = 0.9805). The adsorption capacity value (145 mg/g) calculated from the pseudo-second-order model was close to the experimental value (138 mg/g).

Table 2. Kinetic Parameters of Pseudo-first-order and Pseudo-second-order Kinetic Models for Adsorption of BM on GO/SCB

Pseudo-first-order Model		Pseudo-second-order Model	
k_1 (min^{-1})	0.029	k_2 (g/mg min^{-1})	8.26×10^{-4}
q_e (mg/g)	61.87	q_e (mg/g)	144.93
R^2	0.9805	R^2	0.9996

Adsorption isothermal study

The change of adsorption capacity with the initial concentration of the dye is shown in Fig. 10. When the concentration of BM increased from 5 mg/L to 40 mg/L, the adsorption capacity increased almost linearly. However, while the concentration of BM kept increasing, the adsorption capacity only increased minimally. This indicated that the adsorption almost reached equilibrium and few additional adsorption sites were available for BM. Thus, the initial concentration of BM was set at 30 mg/L.

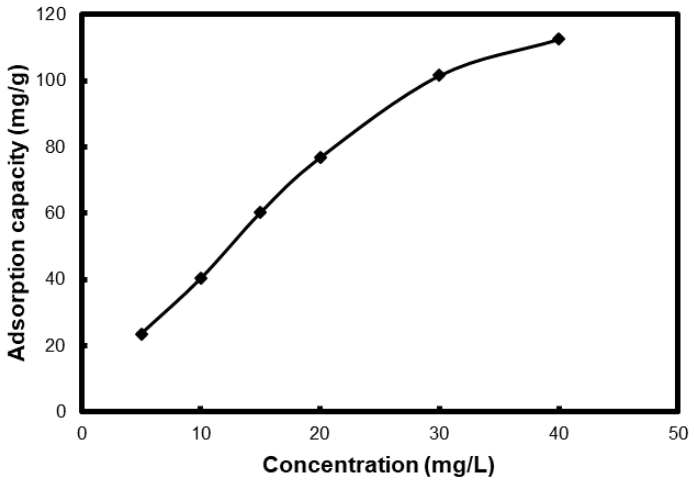

Fig. 10. The variation of the adsorption capacity of graphene oxide/sugarcane bagasse with the initial concentration of BM

To understand the mechanism of adsorption, the Langmuir and Freundlich isotherms (Eqs. 5 and 6) were plotted using the entire concentration range (Sun *et al.* 2018),

$$\frac{C_e}{q_e} = \frac{1}{bQ_0} + \frac{C_e}{Q_0} \quad (5)$$

$$\lg q_e = lgK + \frac{1}{n} lgC_e \quad (6)$$

where C_e is the concentration (mg/L) of the adsorbate at equilibrium, q_e is the adsorption capacity (mg/g) at equilibrium, Q_0 is the maximum adsorption capacity (mg/g) corresponding to complete monolayer coverage on the surface, b is the Langmuir isotherm constant (L/mg), and K and n are the Freundlich isotherm constants ($mg^{1-1/n} L^{1/n}/g$). The plots of C_e/q_e *vs.* C_e and $\ln q_e$ against $\ln C_e$ are given in Figs. 11 and 12, respectively. The

constants of Langmuir and Freundlich isotherm models with the corresponding correlation coefficient value are presented in Table 3.

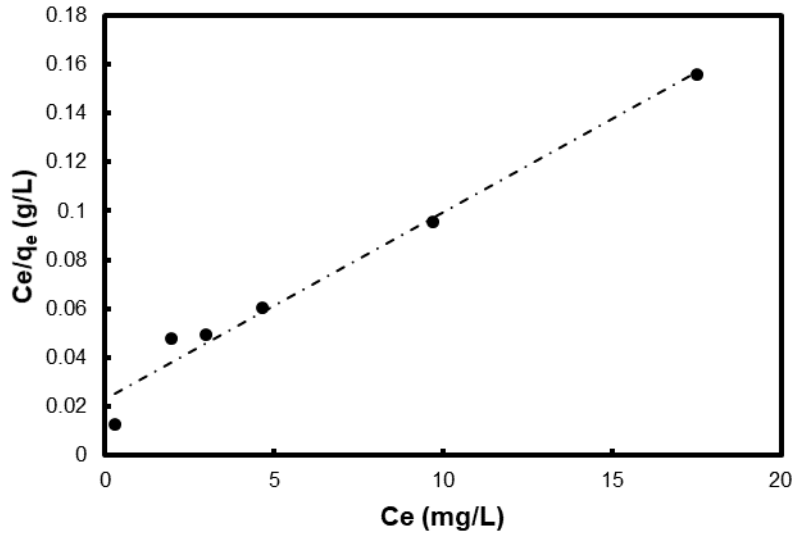

Fig. 11. Langmuir isotherm model for the adsorption of BM on GO/SCB

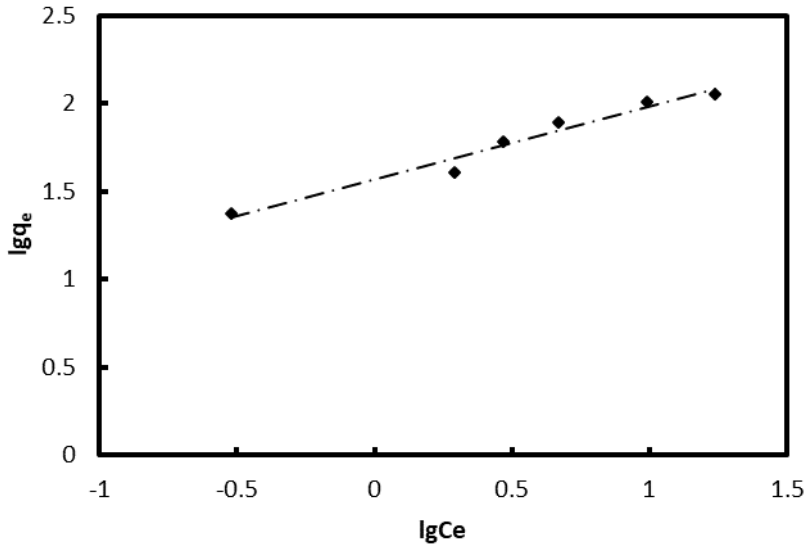

Fig. 12. Freundlich isotherm model for the adsorption of BM on GO/SCB

The value of *1/n* was found to be between 0 and 1 (table 3), indicating that GO/SCB adsorbed BM under the studied conditions. The R^2 value for the Langmuir isotherm (0.9769) was slightly closer to 1.0 than that for the Freundlich isotherm (0.9657). It was assumed that there was the formation of a saturated monolayer of on the surface of the adsorbent and that the adsorption sites had the same energy (Al-Aoh *et al.* 2014).

Table 3. Adsorption Isotherm Constants for Adsorption of BM on GO/SCB

Langmuir Isotherm Constants		Freundlich Isotherm Constants	
b (L/mg)	1.76×10^{-4}	$1/n$	0.41
q_e (mg/g)	131.58	K ($mg^{1-1/n} L^{1/n}/g$)	37
R^2	0.9769	R^2	0.9657

CONCLUSIONS

1. A novel adsorbent was successfully synthesized by modifying sugarcane bagasse using graphene oxide. The adsorbent was characterized using XRD, FTIR, SEM, and TGA. It was concluded that the crystallinity of the fiber decreased and the surface became rough after modification, which was beneficial to the high adsorption.
2. The adsorption ability of sugarcane bagasse and modified sugarcane bagasse was compared and found that the adsorption percentage increased from 55.4% to 99.5% due to modification. The effect of the solution temperature, adsorption time, the initial concentration of the dye, and the amount of the adsorbent was investigated in detail. With 0.03 g of modified sugarcane bagasse, 30 mg/L of BM, and a solution temperature of 60 °C, the adsorption percentage reached 99.5%, and the adsorption capacity was 144.93 mg/g. Graphene oxide-modified sugarcane bagasse showed moderate adsorption performance, which could be potentially applied to the treatment of industrial wastewater.

ACKNOWLEDGMENTS

The authors are grateful for the support of the Education Department of Fujian Province (Grant No. JAT170455), the Fujian Key Laboratory of Textile Fiber and Materials (Grant No. FKLTFM1725), Minjiang University (Grant Nos. 103952018026, MYK17006, MYK 18005), the Fujian Engineering and Research Center of New Chinese Lacquer Materials (Grant No. 323030020102), and the Fujian Provincial University Engineering Research Center of Green Materials and Chemical Engineering (Grant Nos. PY 2018005 and PY 2018006).

REFERENCES CITED

AL-Aoh, H. A., Yahya, R., Maah, M. J., and Abas, M. R. B. (2014). "Adsorption of methylene blue on activated carbon fiber prepared from coconut husk: Isotherm, kinetics and thermodynamics studies," *Desalination and Water Treatment* 52(34-36), 6720-6732. DOI: 10.1080/19443994.2013.831794

Allen, M. J., Tung, V. C., and Kaner, R. B. (2010). "Honeycomb carbon: A review of graphene," *Chem. Rev.* 110, 132-145. DOI: 10.1021/cr900070d

Cheng, J.-S., Du, J., and Zhu W. (2018). "Facile synthesis of three-dimensional chitosan-graphene mesostructures for reactive black 5 removal," *Carbohydrate Polymers* 88, 61-67. DOI: 10.1016/j.carbpol.2011.11.065

Crini, G. (2006). "Non-conventional low-cost adsorbents for dye removal: A review," *Bioresour. Technol.* 97(9), 1061-1085. DOI: 10.1016/j.biortech.2005.05.001

Fideles, R. A., Ferreira, G. M. D., Teodoro, F. S., Adarme, O. F. H., Silva, L. H. M., Gil, L. F., and Gurgel, L. V. A. (2018). "Trimellitated sugarcane bagasse: A versatile adsorbent for removal of cationic dyes from aqueous solution. Part I: Batch adsorption in a monocomponent system," *J. Colloid Interface Sci.* 515(1), 172-188. DOI: 10.1016/j.jcis.2018.01.025

Gan, L., Li, B., Chen, Y., Yu B., and Chen Z. (2019). "Green synthesis of reduced graphene oxide using bagasse and its application in dye removal: A waste-to-resource supply chain," *Chemosphere* (219), 148-154. DOI: 10.1016/j.chemosphere.2018.11.181

Garg, V. K., Kumar, R., and Gupta, R. (2004). "Removal of malachite green dye from aqueous solution by adsorption using agro-industry waste: A case study of *Prosopis cineraria*," *Dyes and Pigments* 62(1), 1-10. DOI: 10.1016/j.dyepig.2003.10.016

Gnansounou, E. (2010). "Production and use of lignocellulosic bioethanol in Europe: Current situation and perspectives," *Bioresour. Technol.* 101, 4842-4850. DOI: 10.1016/j.biortech.2010.02.002

Gupta, V. K., Kumar, R., Nayak, A., Saleh, T. A., and Barakat M. A. (2013). "Adsorptive removal of dyes from aqueous solution onto carbon nanotubes: A review." *Adv. Colloid Interface Sci.* 193-194, 24-34. DOI: 10.1016/j.cis.2013.03.003

Hameed, B. H., and Ahmad, A. A. (2009). "Batch adsorption of methylene blue from aqueous solution by garlic peel, an agricultural waste biomass," *J. Hazard. Mater.* 164, 870-875. DOI: 10.1016/j.jhazmat.2008.08.084

He, Z., Yu, J., Q, Y., and Chi, R. (2013). "PDMA-modified biosorbents for enhancement adsorption of basic magenta," *Environ. Earth Sci.* 70(2), 635-642. DOI: 10.1007/s12665-012-2147-4

Kulal, D. K., Khose, R. V., Pethsangave, D. A., Wadekar, P. H., and Some, S. (2019). "Biomass-derived lignocellulosic graphene composite: Novel approach for removal of oil and organic solvent," *ChemistrySelect* 4, 4568-4574. DOI: 10.1002/slct.201900115

Lee, G., and Kim, B. S. (2014). "Biological reduction of graphene oxide using plant leaf extracts," *Biotechnol. Prog.* 30, 463-469. DOI: 10.1002/btpr.1862

Li, B., Jin, X., Lin, J., and Chen, Z. (2018). "Green reduction of graphene oxide by sugarcane bagasse extract and its application for the removal of cadmium in aqueous solution," *J. Cleaner Prod.* 189, 128-134. DOI: 10.1016/j.jclepro.2018.04.018

Li, B., Gan, L., Owens, G., and Chen, Z. (2018). "New nano-biomaterials for the removal of malachite green from aqueous solution via a response surface methodology," *Water Research* (146), 55-66. DOI: 10.1016/j.watres.2018.09.006

Li, C., Liang, X., and Gu, J. (2017). "Preparation and characterization of bagasse nanocellulose," *Chem. J. Chin. Univ.* 38(7), 1286-1294. DOI: 10.7503/cjcu20160831

Mhamane, D., Ramadam, W., Fawzy, M., Rana, A., Dubey, M., Rode, C., Lefez, B., Hannoyer, B., and Ogale, S. (2011). "From graphite oxide to highly water dispersible functionalized graphene by single step plant extract-induced deoxygenation," *Green Chem.* 13, 1990-1996. DOI: 10.1039/c1gc15393e

Mohammad, F., Arfin, T., and Al-lohedan H. A. (2019). "Enhanced biosorption and electrochemical performance of sugarcane bagasse derived a polylactic acid-graphene oxide-CeO_2 composite," *Mater. Chem. Phys.* (229), 117-123. DOI: 10.1016/j.matchemphys.2019.02.085

Nethravathi, C., and Rajamathi, M. (2008). "Chemically modified graphene sheets produced by the solvothermal colloidal dispersions of graphite oxide," *Carbon* 46, 1994-1998. DOI: 10.1016/j.carbon.2008.08.013

Sophia, A. C., Arfin, T., and Lima, E. C. (2019). "Recent developments in adsorption of dyes using graphene based nanomaterials," in M. Naushad (ed.), *A New Generation Material Graphene: Applications in Water Technology*, Springer, Cham, pp. 439-471.

Srinivasan, A., and Viraraghavan, T. (2010). "Decolorization of dye wastewaters by biosorbents: A review," *J. Environ. Manage.* 91(10), 1915-1929. DOI: 10.1016/j.jenvman.2010.05.003

Sun, N., Wen, X., and Yan, C. (2018). "Adsorption of mercury ions from waste aqueous solution by amide functionalized cellulose from sugarcane bagasse," *Inter. J. Bio. Macro.* 108, 1199-1206. DOI: 10.1016/j.ijbiomac.2017.11.027

Tan, I. A. W., Hameed, B. H., and Ahmad, A. L. (2007). "Equilibrium and kinetic studies on basic dye adsorption by oil palm fiber activated carbon," *Chem. Eng. J.* 127, 111-119. DOI: 10.1016/j.cej.2006.09.010

Vinod, K. G., Rajeev, J., Alok, M., Tawfik, A. S., Arunima, N., Shilpi, A., and Shalini, S. (2012). "Photo-catalytic degradation of toxic dye amaranth on TiO_2/UV in aqueous suspensions," *Mater. Sci. Eng.* 32(1), 12-17. DOI: 10.1016/j.msec.2011.08.018

Xiong, W. (2018). "Bagasse composites: A review of material preparation, attributes, and affecting factors," *J. Thermoplastic Comp. Mater.* 31(8), 1112-1146. DOI: 10.1177/0892705717734596

Yagub, M. T., Sen, T. K., Afroze, S., and Ang, H. M. (2014). "Dye and its removal from aqueous solution by adsorption: A review," *Adv. Colloid Interface Sci.* 209, 172-184. DOI: 10.1016/j.cis.2014.04.002

Zhou, Q., Yan, C., and Luo, W. (2016). "Preparation of a novel carboxylate-rich wheat straw through surface graft modification for efficient separation of Ce(III) from wastewater," *Mater. Design* 97(5), 195-203. DOI: 10.1016/j.matdes.2016.02.081

Article submitted: April 24, 2019; Peer review completed: July 21, 2019; Revised version received and accepted: August 20, 2019; Published: August 22, 2019.
DOI: 10.15376/biores.14.4.8100-8113